Experimental investigation of cavitational bubble dynamics under multi-frequency system

ARTICLE *in* ULTRASONICS SONOCHEMISTRY · MAY 2008

Impact Factor: 4.32 · DOI: 10.1016/j.ultsonch.2007.06.012 · Source: PubMed

2 AUTHORS:

Avvaru Balasubrahmanyam
Institute of Chemical Technology, Mumbai

Aniruddha Pandit
Institute of Chemical Technology, Mumbai

Available online at www.sciencedirect.com
ScienceDirect
ELSEVIER
Ultrasonics Sonochemistry 15 (2008) 578–589
Ultrasonics SONOCHEMISTRY
www.elsevier.com/locate/ultsonch

Experimental investigation of cavitational bubble dynamics under multi-frequency system

Balasubrahmanyam Avvaru, Aniruddha B. Pandit *

Chemical Engineering Division, Institute of Chemical Technology, University of Mumbai, Matunga 400 019, India

Received 17 April 2007; received in revised form 14 June 2007; accepted 25 June 2007
Available online 17 July 2007

Abstract

Acoustic emission spectra measurements have been carried out under mono and multi-frequency acoustic sources to understand the fundamental difference in bubble/cavity dynamics. The effect of introducing the dual and triple frequency acoustic waves of different frequency on the sono-chemical yield has also been investigated experimentally. The introduction of a second wave has increased the number of cavitating bubbles and as well as the collapsing intensity of cavities resulting into higher sono-chemical yield, and better effective utilization of reactor volume with a large number of resonating cavitating bubbles. To get the information about the intensity of each of the cavity oscillating events, decomposition of the pressure signal measured by the hydrophone in the frequency domain of the FFT power spectrum has been carried out. Inverse fourier reconstruction technique, has been used to elaborate the dynamics of the cavitating bubbles in the multi-frequency system.

Keywords: Acoustic emission spectra; Multiple frequency; FFT power spectrum; Cavitational bubbles; Sono-chemical yield

1. Introduction

Bubbles are fascinating in their own right, from the most innocent-looking problem of a rising bubble in still water to their formation, oscillation, and collapse. A bubble collapse can be extremely violent, as revealed in light emission, so called sonoluminescence [1]. In nature some shrimps use the very high energy of this bubble collapse to kill prey [2], and many technological applications such as ultrasonic cleaning and sono-chemical transformations also utilize it.

Ultrasound as a means of introducing energy in a medium to bring about a chemical/physical change through the phenomena of bubble collapse has been investigated extensively over the past several years [3–6]. The basic physical phenomena behind all physical, chemical and biological effects of ultrasound, is cavitation. High temperature-pressure pulse resulting from the collapse of the transient cavitation bubbles is responsible for all the observed mechanical/physical effects of ultrasound. The major short coming of the ultrasound reactor is that cavitation occurs only in the close vicinity of the surface of the transducer and severely limits the active volume of the reactor and this leads to poor performance on industrial scale operations. In order to overcome these difficulties researchers working in the field of engineering sono-chemistry have successfully applied multi-frequency acoustic sources in enhancing the sono-chemical yield. Iernetti et al. [7] studied the cavitational effects given by a high-frequency pulsed ultrasound field with and without the superimposed stimulation by a low frequency field. Sonoluminescence intensity and subharmonic intensity of the high-frequency field were measured. The stimulation of a cavity by a low frequency field gives a sharp rise in both subharmonic and sonoluminescence intensities. Swamy et al. [8] successfully applied dual frequency acoustic sources in enhancing the metal leaching rates and the final recovery values of the metals. Feng et al. [9] found that the multiple frequency irradiation of ultrasound has a significant increase in the cavitational

* Corresponding author. Tel.: +91 22 4145616; fax: +91 22 4145614.
E-mail address: abp@udct.org (A.B. Pandit).

1350-4177/$ - see front matter © 2007 Elsevier B.V. All rights reserved.
doi:10.1016/j.ultsonch.2007.06.012

yield compared to mono frequency irradiation. Wang et al. [10] studied the sono-chemical enhancement of the degradation of pentachlorophenol with multiple frequency acoustic system. Gogate et al. [11] studied the degradation of formic acid using horn and bath type (mono and multi-frequency) reactors. They have compared these type of equipments using the two characteristic parameters, i.e. energy efficiency (net energy dissipated/electrical energy supplied) and the cavitational yield they have concluded that the multi-frequency irradiation was more efficient in the destruction of formic acid.

Thus, it is important to understand the effect of multi-frequency operation on the resultant acoustic pressure fields generated and its effects on the bubble dynamics for the design of a sono-chemical reactor. With this view Mohalkar et al. [12] have numerically investigated the enhancement in cavitational yield with the dual frequency acoustic processor and proposed, that the enhancement is due to the presence of a more uniform acoustic field in the processor. They also provided a methodology for optimizing the condition of the dual frequency acoustic field for the generation of a uniform cavitational intensity in the reactor. Numerical studies of Tatake et al. [13] suggest that the introduction of the second acoustic wave of the same frequency of that of the first wave is expected to give maximum cavitational enhancement. Prabhu et al. [14] studied the effect of operating parameters such as frequency, initial radius of the cavities, gas content and temperature on the net cavitational yield in a triple frequency sono-chemical reactor using numerical simulation of cavity dynamics equations, and suggested the best combination of operating parameters for the higher cavitational yield. Servent et al. [15] in their numerical modeling, considered both the nucleation sites and spatial/temporal dynamics of the cavitation bubbles in a three-dimensional geometry of the sono-chemical reactor and concluded that the cavitational bubble volume fractions are higher (indicating possibly larger number of cavitational events under dual frequency than under mono frequency sources) in multi-frequency system.

In the present work, the experimental investigation of bubble dynamics by using acoustic emission spectra measurements under the multiple frequency sources have been carried out to understand the effect of multi-frequency ultrasound irradiation on the cavity dynamics, subsequent cavitational effects, and also the uniform acoustic pressure field obtained by the elimination of the inactive regions (standing waves pattern) of the pressure field. Based on these acoustic emission spectra measurements of the multi-frequency irradiation the best combination for the maximum enhancement in the cavitational yield has been proposed. To find out whether these measurements are feasible in actual sono-chemical processes a model reaction of aqueous potassium iodide (KI) decomposition has been chosen and the yields obtained under irradiation have been compared with the resultant acoustic emission spectra measurements under multi-frequency operation.

2. Experimental work

Experiments are carried out in a triple frequency ultrasonic hexagonal bath system consisting of six sides, each of the two opposite sides are fitted with the same ultrasonic frequency transducers 41.5 kHz, 30 kHz and 25 kHz, respectively. Each side is fitted with single transducer. Each of the face width is 10 cm and depth of the hexagonal bath is 30 cm. Schematic representation of the experimental set up is shown in the Fig. 1. The acoustic emission spectra measurements were carried out with a small hydrophone (Bruel & Kjear Ltd., Type 8103) connected to a charge amplifier (Bruel & Kjear Ltd., Type 2635). The output of this amplifier was fed to a computer, equipped with data acquisition system (N.I. Ltd., PCI 6251) and the discrete data has been captured, FFT power spectrum analysis has been carried out with online FFT power spectrum analysis using graphical interface programming done with the Labview software (N.I. Ltd. Version 7.1). The temperature of water in all the experiments were maintained in the range of 30–32 °C. To avoid any significant rise in the temperature the bath was operated intermittently with a short duration of the irradiation. This hexagonal bath can be operated in 7 different modes through seven different channels. Channel 1 operates at 41.5 kHz, channel 2 operates at 30 kHz, channel 3 operates at 25 kHz, channel 4 operates with 30 and 41.5 kHz, channel 5 operates with 25 and 41.5 kHz, channel 6 operates with 25 and 30 kHz, and channel 7 operates with all these three frequency transducers irradiating simultaneously. The measurements with hydrophone were taken at a depth of 7.5 cm from the top, all the measurements have been taken at the same location. The signal coming from the hydrophone is amplified with the help of a charge amplifier and then fed to the computer for data acquisition. The discrete data of the samples were taken at a sampling frequency rate of 360 kHz, and each signal consisted of 16384 digital points. Since the two consecutive cavitational events are random in nature, 50 of such pressure signals

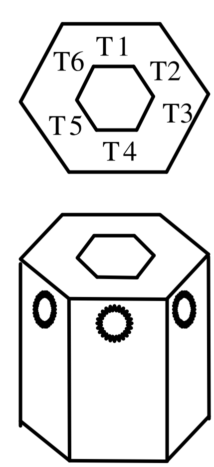

Fig. 1. Hexagonal multi-frequency ultrasonic bath.

were analyzed to get the rms average of FFT power spectra.

2.1. Analysis of data

The pressure signal measured by the hydrophone is due to bubble activity. Oscillating bubble acts as a secondary source of sound. The impingement of micro-jets produced by the asymmetrically collapsing cavitational bubbles is as a result of due to asymmetric environment created by the presence of the hydrophone. Different peaks in the FFT power spectrum of the measured pressure signal give the information about the subharmonic, harmonic and ultra harmonically oscillating cavitational bubbles. The collective pressure pulse from the bubbles, which corresponds to any one particular frequency can be obtained by decomposing the signal in the frequency domain of the FFT spectrum and then reconstructing it at those particular frequencies by inverse Fourier reconstruction technique; this procedure of reconstruction of inverse FFT is well explained in our earlier work [16]. For this operation of FFT power spectrum decomposition and the inverse FFT reconstruction, Autosignal version 1.7 software package (Systat software Ltd.) has been used. A brief algorithm indicating the sequence of mathematical operation during the analysis of the data has been given in our earlier work [16].

3. Results and discussions

3.1. Bubble dynamics under single frequency

Earlier researchers have explained several characteristics of the acoustic emission spectra of the single transducer system. It is generally known that the acoustic cavitation noise spectrum comprises of various frequencies related to the fundamental or the driving frequency. These frequencies are either the subharmonic (f/n), the harmonic (nf) and ultra harmonic ($(2n+1)f/2$) of the fundamental driving frequency 'f'. The higher harmonics in the acoustic emission spectrum are explained in terms of the forced non-linear bubble oscillations and the noise background is explained in terms of the shock waves emitted by the collapsing bubbles.

The first detailed explanations of the subharmonics were given by Guth [17], which were later confirmed by Neppiras [18,19], Eller and Flynn [20]. Guth [17] demonstrated that a bubble with an equilibrium radius greater than the resonance value would pulsate and as a consequence would radiate the subharmonic frequencies. Another possible explanation for the subharmonic emission was given by Akulichev [21], He demonstrated that because of the inertial forces (when the pressure amplitude of the ultrasound exceeds a certain threshold) a bubble expands even during the compression half-period and passes the contraction phase. As a result, the time period of the pulsation of the bubble becomes a double of the period of the ultrasound and the subharmonic components appear in the acoustic emission spectra. Similarly, Apfel [22], showed that the transient cavitation could be characterized by the bubbles that survive for more than one acoustic cycle and repeat the form of radial motion as in the first cycle. This type of motion can generate the sub-harmonic emission.

When only one acoustic frequency is in operation, the ultrasound wave coming from the acoustic source (transducer) forms a simple harmonic wave, which after getting reflected at the opposite reactor wall (or the top liquid surface in ultrasonic bath) can give rise to a standing wave pattern. In the case of the two sources operating at the same frequencies, the acoustic field comprises of the waves of the same\frequency coming from the two opposite sides, and the resultant pressure signal measured by the hydrophone under the frequency of 41.5 kHz placed opposite to each other is shown in the Fig. 2a. The FFT power spectrum of the driving frequency has been decomposed in its frequency domain to get the information about the pressure associated with the driving frequency and the resulting cavitational intensities. These pressure intensities are shown in the Fig. 2b and c, respectively. The average strength of the signal is represented in terms of the rms value of the pressure signal, and is mentioned in each of the figures. Similarly, for the other pair of mono frequency transducers of 30 and 25 kHz, pressure signals measured by the hydrophone and their inverse FFT reconstructed

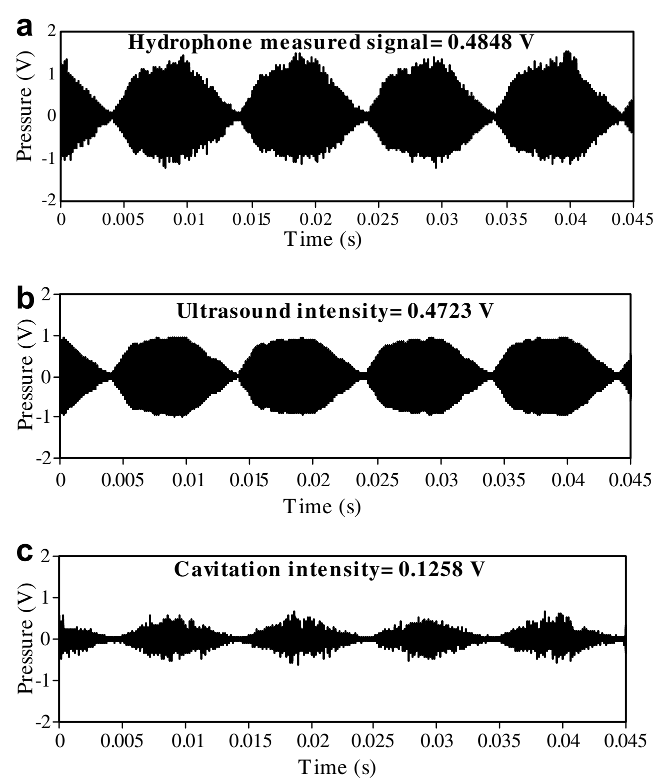

Fig. 2. (a) Hydrophone measured pressure signal of channel 1. (b) FFT reconstructed pressure signal of ultrasonic intensity of channel 1. (c) FFT reconstructed pressure signal of cavitation intensity of channel 1.

pressure intensity components are shown in the Figs. 3 and 4, respectively. The driving acoustic wave of each transducer undergoes some period of modulation. This modulation of each transducer in the bath was measured to have a frequency of 100 Hz. The cause for the ultrasound modulation lies in the electrical design of the signal generator [23]. The corresponding average FFT power spectrum of 50 measured pressure pulses of each of the channel 1 (41.5 kHz), channel 2 (30 kHz) and channel 3 (25 kHz) is shown in the Fig. 5a–c, respectively, showing the peaks at sub-harmonics, harmonics and ultra-harmonics of the driving frequencies in the frequency domain of FFT power spectrum, which was found to be similar to the FFT power spectrum obtained from a single acoustic source of frequency 20 kHz [16]. This shows that the observed acoustic emission spectra does not change under two acoustic sources of same frequency operating in opposite direction to each other.

Even though, each of the three different frequency transducer have the same power rating (150 W mentioned by the manufacturer) the rms values of the measured pressure signals are different. This variation is evident, since the hydrophone measures the oscillating action of the cavities and the collapse events rather than the rated power intensity of each transducer. With 41.5 kHz driving frequency transducers the rms value measured by the hydrophone is high (0.485 V) as compared to the 30 kHz (0.332 V) and 25 kHz (0.197 V) as driving frequencies. Similarly, the FFT reconstructed ultrasonic intensities for these driving frequencies are 0.472, 0.287 and 0.144 V, respectively. This essentially indicates the energy efficiency of each of these transducer sets. It appears that, even though 150 W of electrical power is consumed by the transducer, the actual delivered power is different. The corresponding cavitational intensities are 0.126, 0.167 and 0.134 V, respectively, indicating that the 30 kHz transducer produces the maximum net cavitational activity.

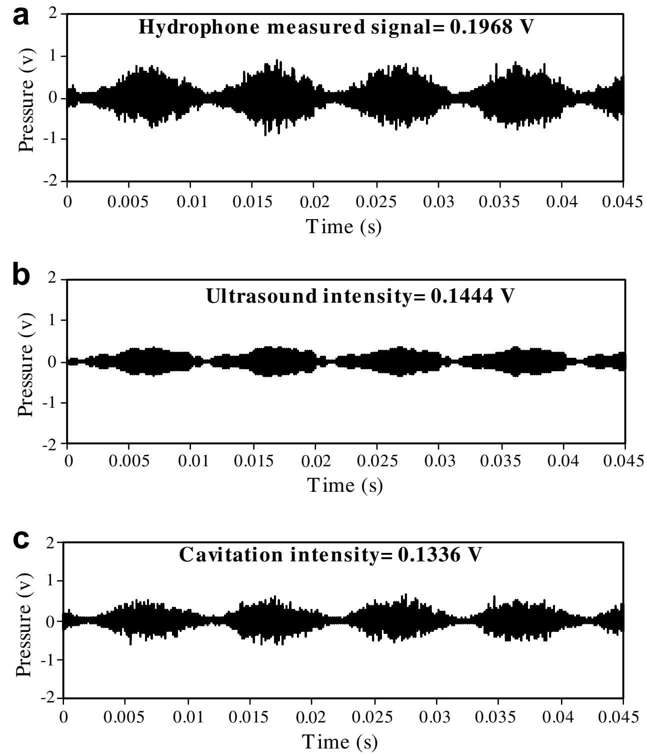

Fig. 4. (a) Hydrophone measured pressure signal of channel 3. (b) Inverse FFT reconstructed pressure signal of ultrasonic intensity of channel 3. (c) Inverse FFT reconstructed pressure signal of cavitation intensity of channel 3.

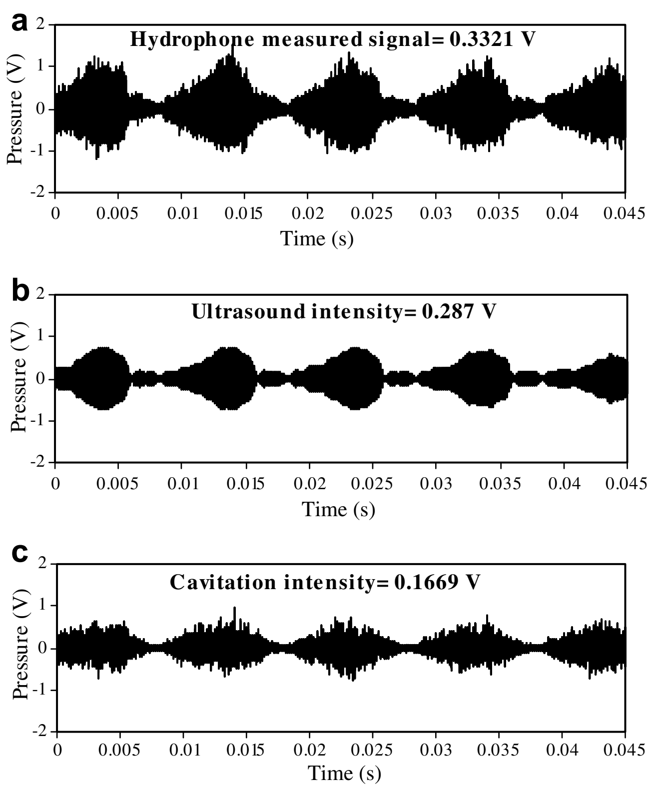

Fig. 3. (a) Hydrophone measured pressure signal of channel 2. (b) Inverse FFT reconstructed pressure signal of ultrasonic intensity of channel 2. (c) Inverse FFT reconstructed pressure signal of cavitation intensity of channel 2.

Aluminium foil erosion measurements studies have been conducted in order to qualitatively estimate the distribution of the acoustic pressure field under a mono frequency transducer arrangement (i.e. channel 2, 30 kHz). The measured erosion pattern on the foil shown in the Fig. 6, indicate a series of bands of active zones of cavitation causing the indentations/erosion of the aluminium foil. The active cavitational zones forming as a result of standing wave formation within the reactor, after the reflection of the driving sound wave from the opposite side of the walls of the reactor. Bjerken's forces acting on the oscillating cavitational bubbles causes the accumulation of the bubbles at the anti-nodal regions (high amplitude pressure zones) and their subsequent collapse giving a series of erosion bands on the aluminium foil. This indicates the active and inactive zones of cavitation under mono frequency transducer arrangement.

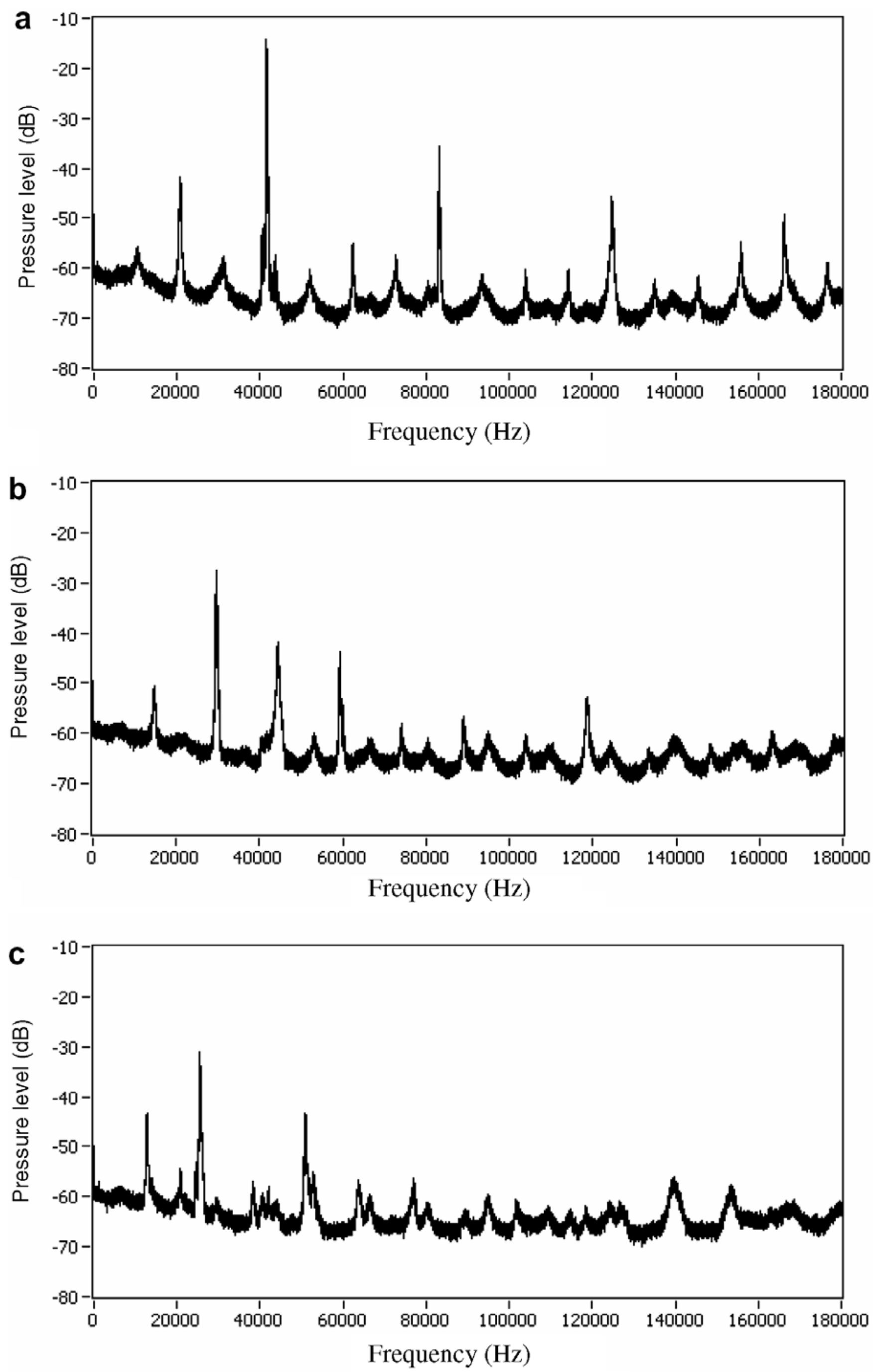

Fig. 5. (a) FFT power spectrum of channel 1 (41.5 kHz). (b) FFT power spectrum of channel 2 (30 kHz). (c) FFT power spectrum of channel 3 (25 kHz).

3.2. Bubble dynamics under multiple frequency sources

Bubble dynamics, in terms of acoustic emission spectra under multi-frequency transducers have been measured with the existing data acquisition system. The average FFT power spectrums of 50 measured pressure pulses of these (channels 4, 5 and 6) multi-frequency operations are shown in the Fig. 7. These FFT power spectra show quite a number of interesting peaks in the frequency domain, indicating that quite distant events are occurring at some regular frequencies other than the sub-harmonics, harmonics and ultra-harmonics of each of the individual driving frequencies. The explanation for the occurrence of these events is not simple at the present stage of analysis. However, some researchers [24–27] have offered some plausible explanations for these events. When bubbles are put into forced oscillations by a low frequency (f_r) field and are simultaneously superimposed by a higher frequency (f_o) oscillating pressure field, the observed spectra will contain side bands at $f_o \pm f_r$ as well as higher order

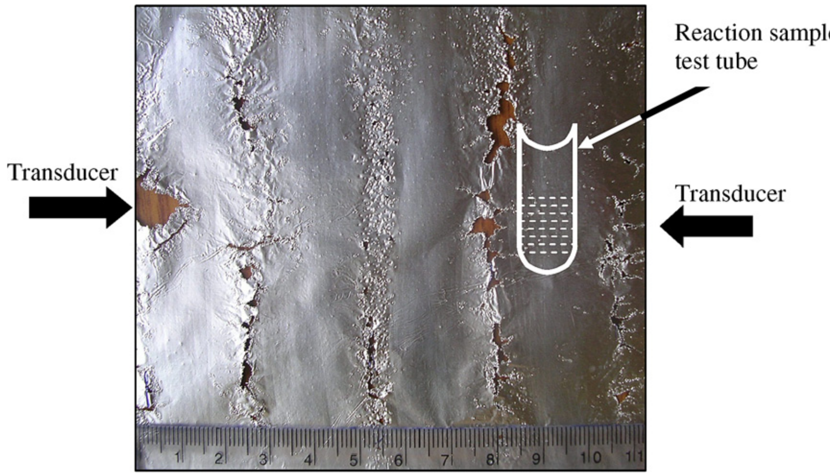

Fig. 6. Aluminium foil erosion measured under Channel: 2 (30 kHz).

frequency terms. Even though, in the present work, the two driving frequencies employed are in the same range (variation is less than one order of magnitude), one can still identify differently oscillating cavities under multi-frequency operation based on the obtained average FFT power spectrum. To quantify the cavitational activity associated with these events, the inverse FFT reconstruction technique has been used to reconstruct the pressure signal at these different frequencies. To compare the resultant of the dual frequency transducer arrangement with the single frequency irradiation, 30 and 41.5 kHz driving frequencies with mono as well as dual frequency irradiation were chosen as a typical case. The pressure signal measured by the hydrophone, as well as the inverse FFT reconstructed pressure signals at each of these regularly oscillating cavitational events, at different frequencies in the frequency domain are shown in the Fig. 8. The rms values of the pressure signal given by the hydrophone of the simultaneous irradiation of these two frequency sources was about 0.58 V. The ultrasonic and resultant cavitational (bubble oscillation) intensity pressures are 0.522 and 0.257 V, respectively. This suggests a significantly higher value of cavitational intensity (0.257 vs. 0.126 V) under simultaneous dual frequency application, and this value is nearly 2 times more than 41.5 kHz individual driving frequency and 1.5 times more than the 30 kHz individual driving frequency operations. As we can observe from the Fig. 7a, the frequency of different oscillating events (in the FFT spectrum) is 12.2, 20, 47, 53, 59, 66, 71, 83, 95, 100, 112, 124 and 139 kHz. These inverse FFT reconstructed pressure signals are shown in the Fig. 8, and the corresponding rms values of these oscillating events are 0.082, 0.026, 0.043, 0.109, 0.021, 0.027, 0.057, 0.083, 0.063, 0.014, 0.023, 0.031 and 0.021 V, respectively at the corresponding frequencies. These are substantially different oscillating events compared to the observed harmonics and ultra-harmonics of the each of the individual single frequency irradiations as shown in the Fig. 5a and b. The two other different multi-frequency combinations such as channel 5, channel 6 and their corresponding rms values of the inverse FFT reconstructed pressure signal at each of the different frequencies of bubble oscillation are shown in the Tables 1 and 2, respectively. Similarly, the FFT power spectrum of triple frequency irradiation of all the three driving frequencies of 41.5, 30 and 25 kHz (channel 7) are shown in the Fig. 9. The inverse FFT reconstructed pressure signals at each of the oscillating frequencies of the bubble/cavity events are shown in the Fig. 10. The rms values of the pressure measured by the hydrophone, ultrasonic and cavitational intensities are found to be in the range of 0.603, 0.489 and 0.344 V, respectively. Introduction of 25 kHz frequency to the dual frequency source of 41.5 and 30 kHz indicates further enhancement in the cavitational intensity by 33% (1.33 times). The number of different oscillating events that are occur in the frequency domain of its FFT spectrum are at 12.2, 20, 47, 53, 55, 59, 62, 66, 71, 83, 95, 100, 112, 118, 124 and 139 kHz and the corresponding rms values of these oscillating events are 0.072, 0.145, 0.036, 0.102, 0.075, 0.043, 0.035, 0.045, 0.057, 0.053, 0.047, 0.02, 0.032, 0.029, 0.039, 0.057 V, respectively.

Aluminium foil erosion measurements studies have been conducted in order to estimate the distribution of acoustic pressure field and the subsequent cavitation fields under dual and triple frequency transducer arrangement. The measured erosion foil under dual frequency (channel 4: 41.5 + 30 kHz) and triple frequency (channel 7: 41.5 + 30 + 25 kHz) have been shown in the Figs. 11 and 12, respectively. The observed uniform erosion pattern indicates the reduction and/or elimination of inactive zones (clear bands) of cavitation observed in the case of single frequency transducer system. The introduction of third source at an angle (as it is a hexagonal arrangement) to the primary transducer source has given even a more uniform pressure field, which makes the entire reactor volume

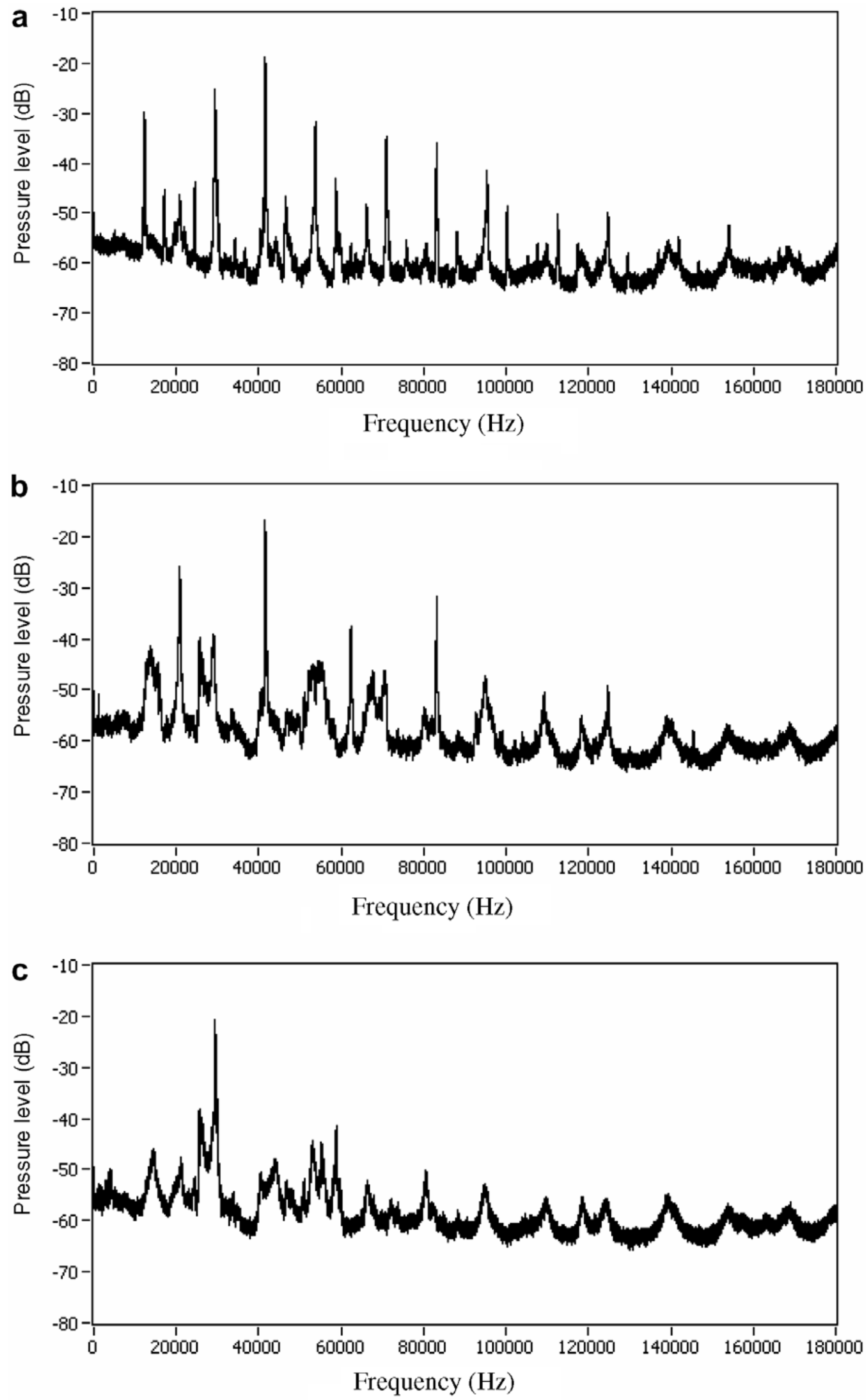

Fig. 7. (a) FFT power spectrum of channel 4 (41.5 + 30) kHz. (b) FFT power spectrum of channel 5 (25 + 41.5) kHz. (c) FFT power spectrum of channel 6 (25 + 30) kHz.

operate with active cavitation and causes more intense erosion as can be observed from the Fig. 12. The observation of each of the FFT power spectrums under simultaneous application of multi-frequency irradiation, Figs. 7 and 9 indicates a substantially different number of oscillating events at different oscillating frequencies showing an increase in the number of non-linearly oscillating bubbles/cavities over a wide spectrum of resonating bubble radii and the intensities of their collapse.

4. Experimental quantification of sono-chemical yield

The cavitational yield (sono-chemical yield) can be directly related to the collapse pressures and the number of cavity collapsing events [28]. Hence, it was decided to quantify experimentally how the introduction of the second and third frequency sound wave will affect the sono-chemical yield as compared to a single frequency operation. The model reaction of potassium iodide (KI) decomposition

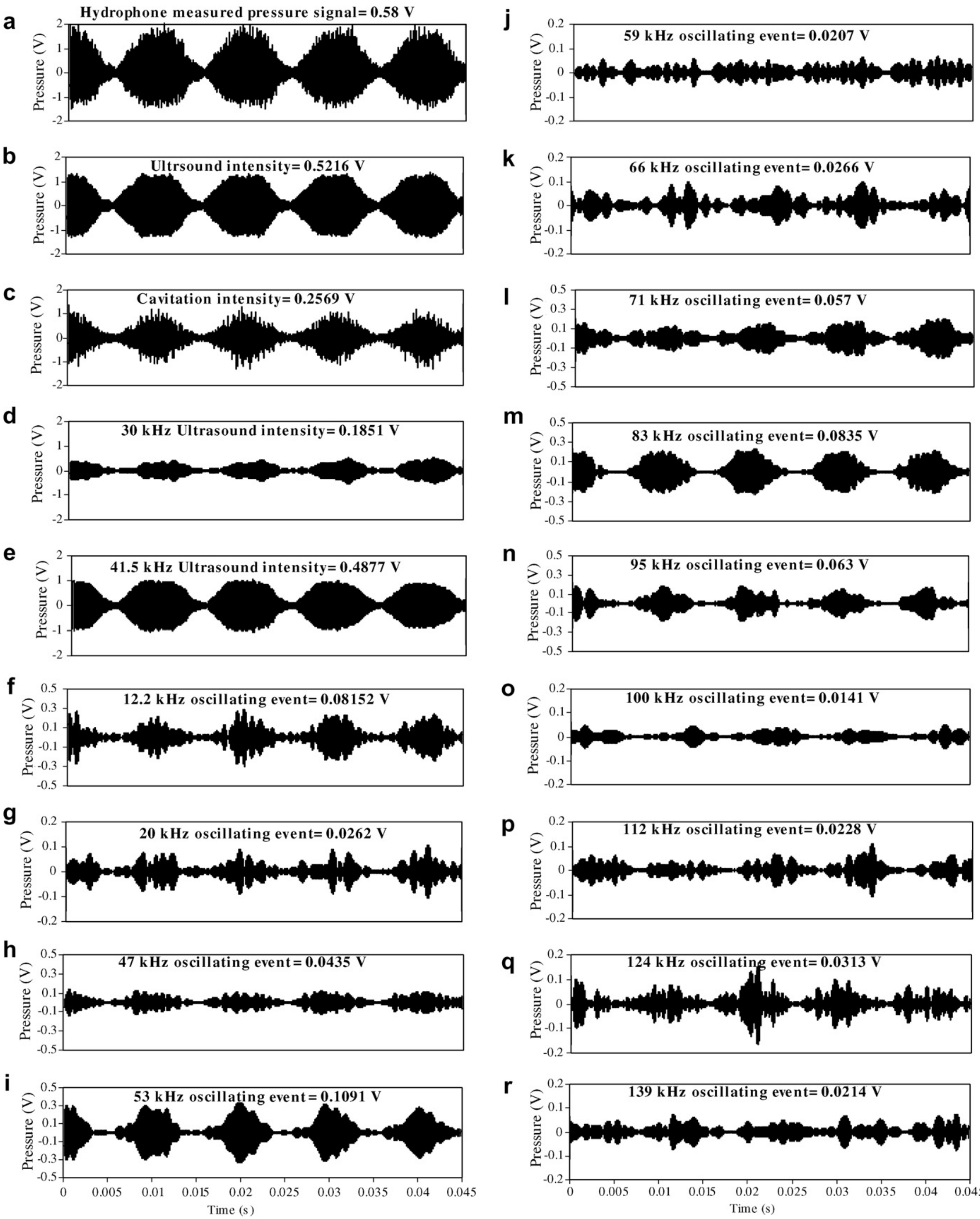

Fig. 8. Inverse FFT reconstructed pressure signals of different oscillating events of channel 4 (41.5 + 30) kHz.

(Weissler's reaction) [29,30] has been considered for this quantification. A small test tube was kept at a depth of 7.5 cm below the upper surface, exactly where the acoustic emission spectra measurements were taken. Each time

Table 1
Channel 5; (25 + 41.5) kHz

S. No.	Frequency event (kHz)	rms values (V)
1	13	0.068
2	20.8	0.264
3	25.5	0.118
4	28.8	0.095
5	45.0	0.475
6	47.0	0.034
7	53.0	0.072
8	62.0	0.071
9	67.0	0.072
10	70.5	0.038
11	83.0	0.093
12	88.5	0.015
13	95.0	0.043
14	110.0	0.039
15	118.0	0.020
16	124.0	0.022
17	139.0	0.023

Table 2
Channel 6; (25 + 30) kHz

S. No.	Frequency event (kHz)	rms values (V)
1	5.0	0.034
2	15.0	0.065
3	20.0	0.043
4	25.0	0.110
5	30.0	0.502
6	44.0	0.060
7	53.0	0.057
8	55.0	0.069
9	59.0	0.088
10	80.5	0.047
11	94.5	0.033
12	110.0	0.025
13	118.0	0.026
14	124.0	0.021
15	139.0	0.028

5 mL of 5% KI solution was placed in a test tube, which was then immersed in the ultrasonic hexagonal bath and irradiated for 12 min. Samples were analyzed for iodine (I_2) liberation immediately (amount of iodine released was measured at the absorbance wavelength of 355 nm using a UV–Vis Spectrophotometer, Chemito model-2500, India). Same set of experiments have been carried out under the different channels of operation; 1–7. The experiments were carried out twice and average values have been reported. The average iodine liberated per unit amount utilized energy have been reported in the Table 3. As can be observed from the Fig. 13, the decreasing rate of iodine liberation (normalized in terms of total energy dissipation) under these channels are channel 5 > channel 7 > channel 4 > channel 6 > channel 2 > channel 3 > channel 1. The trend is similar to the trend of cavitational intensities of the acoustic emission spectra measurements. The increase in the sono-chemical yield under multi-frequency irradiation is not only due to the increase in number of different resonating cavities, but also due to uniform acoustic pressure field distribution observed through out the reaction sample volume which is quite evident from the uniform erosion on the aluminum foil observed under different frequency combination of operation, which is shown in the Figs. 11 and 12. The comparison between Figs. 8 and 10 along with Figs. 11–13 shows a direct correspondence between the pressure signal measured by the hydrophone and the sono-chemical yield.

However, our previous work (Tatake et al. [13]; Gogate et al. [31]) has reported that in the case of a ultrasonic bath type reactor the cavitational yield is a function of location of the reaction sample in the bath as a result of the formation of standing waves and due to the presence of varying sound pressure field our experiments with the single frequency operation has also confirmed it (erosion bands shown in Fig. 6). The location where the nodes are formed shows very less cavitational activity, and the location where anti-nodal points exists show high cavitational activity (it is nearly 2.6 times more, Tatake et al. [13]), even though the intensity of ultrasound at this location is lower as compared to the intensity at transducer surface due to the

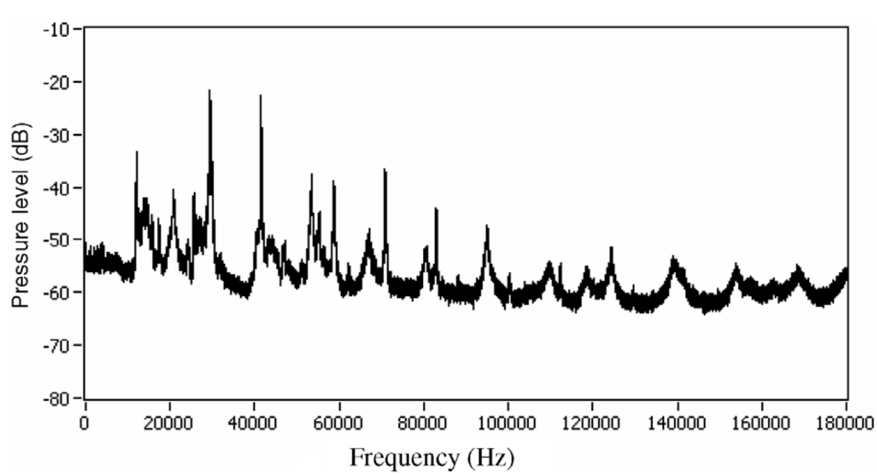

Fig. 9. FFT power spectrum of channel 7 (41.5 + 30 + 25) kHz.

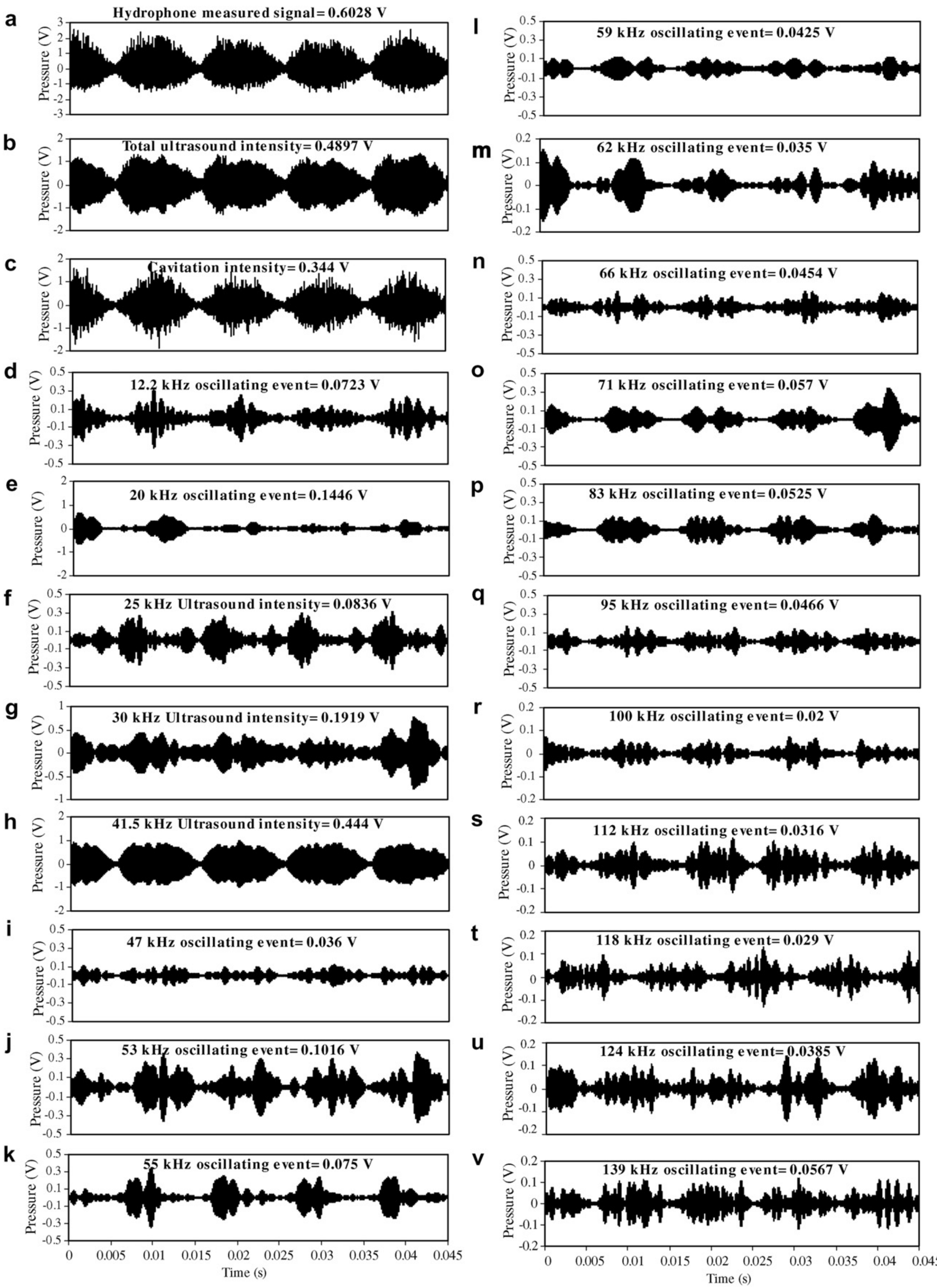

Fig. 10. Inverse FFT reconstructed pressure signals of different oscillating events of channel 7 (41.5 + 30 + 25) kHz.

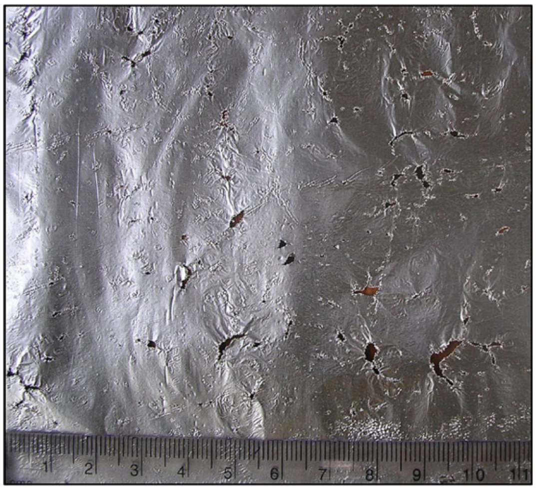

Fig. 11. Aluminium foil erosion measured under dual frequency (41.5 + 30) kHz.

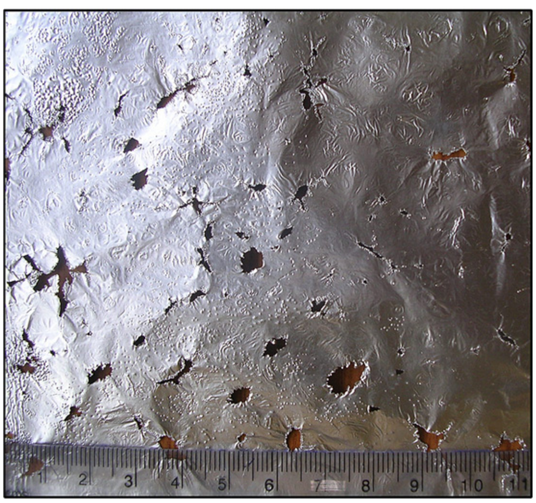

Fig. 12. Aluminium foil erosion measured under triple frequency (41.5 + 30 + 25) kHz.

Table 3
Normalized sono-chemical yield

S. No.	Channel	Sono-chemical yield per unit energy dissipated per unit volume ($\times 10^6$ gm/L/Watt)
1	1	6.67
2	2	60.0
3	3	13.3
4	4	400.0
5	5	518.0
6	6	257.0
7	7	432.0

attenuation of the sound during its propagation from the source surface.

In the present analysis, the reaction sample was kept at a nodal region (it is clearly shown in the aluminum erosion pattern observed under channel 2 at the central location of 8.75 cm from the left transducer surface in the bath, shown in the Fig. 6), and hence the observed sono-chemical yield is low in the case of single frequency operation. Similarly under channels 1 and 3, the position of the reaction sample was at the nodal region. With the use of the second frequency these low cavitational activity bands (nodes showing no erosion) get eliminated and over all cavitational activity increases. Hence, the dual frequency operation has the synergetic effect in enhancing the sono-chemical yield compared to single frequency irradiations. It clearly suggests that the one should dissipate the energy with two or more transducers simultaneously for synergetic effects to get enhanced sono-chemical yield at equivalent levels of overall power dissipation.

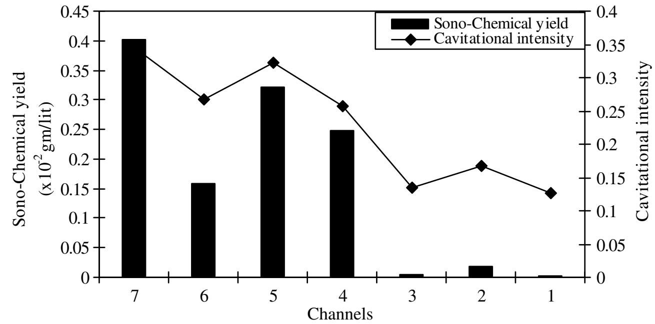

Fig. 13. Comparison of sono-chemical yield with the cavitation intensity measured with the acoustic emission spectra.

5. Conclusion

In the present work, the experimental investigation of bubble dynamics based on the acoustic emission spectra measurements under the multiple frequency acoustic sources have been carried out to understand the effect of multi-frequency ultrasound irradiation on the cavity dynamics and its subsequent effect on cavitational yield. The introduction of the second and third acoustic waves of different frequencies increases the measured pressure intensity by the hydrophone. An increase in the sono-chemical yield has been observed, indicating the catastrophic collapse of the cavities yielding higher cavitational effects. The different oscillating peaks observed in the FFT power spectrum under multi-frequency operation indicate a broad range of cavitating bubbles oscillating with their resonating frequencies. Aluminium foil erosion measurement studies have shown that the introduction of the second and third acoustic waves eliminates the inactive zones of cavitation at nodal points of the acoustic pressure field, showing that active uniform cavitation extends throughout the reactor volume, making effective utilization of the acoustic cavitational reactor.

Acknowledgement

The authors acknowledge the funding of Department of Atomic Energy, Govt. of India. For this collaborative research work under the project name DAE-KBE, Project Number: 47.01.12. One of the author Avvaru. B., conveying special thanks to Dr. (Mrs.) S.B. Roy, U.E.D., B.A.R.C., for timely encouragement and for giving the permission to publish this research work. Authors would also like to acknowledge Prof. V.D. Deshpande (Physics departments, ICT, Mumbai) for reading the manuscript and giving the helpful suggestions.

References

[1] M.P. Brenner, Hilgenfeldt, D. Lohse, Rev. Mod. Phys. 74 (2002) 425.

[2] D. Lohse, M. Versluis, A. Heydt, B. Schmidt, Science 289 (2000) 2114.

[3] T.J. Mason, Chemistry with Ultrasound, Elsevier Applied Science, 1986.

[4] T.J. Mason, J.P. Lorimer, Sonochemistry: Theory Applications and uses of Ultrasound in Chemistry, Ellis Horwood, Chichester, 1989.

[5] T.J. Mason, J.P. Lorimer, Applied Sonochemistry. The Uses of Power Ultrasound in Chemistry and Processing, Wiley VCH, Weinheim, 2002.

[6] K.S. Suslick, Ultrasound: its Chemical Physical and Biological Effects, VCH Publishers, 1988.

[7] G. Iernetti, P. Ciuti, N.V. Dezhkunov, M. Reali, A. Francescutto, G.K. Johri, Ultrason. Sonochem. 4 (1997) 263–268.

[8] K.M. Swamy, K.L. Narayana, Ultrason. Sonochem. 8 (2001) 341.

[9] R. Feng, Y. Zhao, C. Zhu, T.J. Mason, Ultrason. Sonochem. 9 (2002) 231.

[10] S. Wang, H. Bingbing, W. Yansong, L. Li, Ultrason. Sonochem 13 (6) (2006) 506–510.

[11] P.R. Gogate, S. Mujumdar, A.B. Pandit, Adv. Environ. Res. 7 (2003) 283–299.

[12] V.S. Moholkar, R.M. Sander, M.C.G. Warmoeskerken, Ultrasonics 38 (2000) 666–670.

[13] P.A. Tatake, A.B. Pandit, Chem. Eng. Sci. 57 (2002) 4987–4995.

[14] A.V. Prabhu, P.R. Gogate, A.B. Pandit, Chem. Eng. Sci. 59 (2004) 4991–4998.

[15] G. Servent, J.L. Laborde, A. Hita, J.P. Caltagirone, A. Gerard, Ultrason. Sonochem. 10 (2003) 347–355.

[16] B. Avvaru, A.B. Pandit, Under Rev. J. Acous. Soc. Am. (2007).

[17] W. Guth, Acustica 6 (1956) 532–538.

[18] E.A. Neppiras, J. Acous. Soc. Am. 46 (1969) 587–601.

[19] E.A. Neppiras, J. Sound Vib. 10 (1969) 176.

[20] A. Eller, H.G. Flynn, J. Acous. Soc. Am. 46 (1969) 722–727.

[21] V.A. Akulichev, Akusticheskii J. 13 (1967) 533 (in Russian).

[22] R.E. Apfel, in: P.D. Edmonds (Ed.), Methods in Experimental Physics, Vol. 19, Academic Press, New York, 1981.

[23] V.S. Moholkar, M. Huitema, S. Rekveld, M.M.C.G. Warmoskerken, Chem. Eng. Sci. 57 (2002) 617–629.

[24] V.L. Newhouse, P.M. Shankar, J. Acoust. Soc. Am. 75 (1984) 1473.

[25] P.M. Shankar, J.Y. Chapelton, V.L. Newhouse, Ultrasonics 24 (1986) 333.

[26] T.G. Leighton, R.J. Lingard, A.J. Walton, J.E. Field, Ultrasonics 29 (1991) 319.

[27] A.D. Phelps, T.G. Leighton, in: L. Bjorno (Ed.), Proceedings of the 3rd European Conference on Underwater Acoustics, 1994, pp. 201.

[28] P.R. Gogate, A.B. Pandit, AICHE J. 46 (2) (2000) 372–379.

[29] P.R. Gogate, I.Z. Shirgaonkar, M. Sivakumar, P. Senthil kumar, N.P. Vichare, A.B. Pandit, AICHE J. 47 (2001) 2526.

[30] K.S. Suslick, M.M. Mdleleni, J.T. Reis, J. Am. Chem. Soc. 119 (1997) 9303.

[31] P.R. Gogate, P.A. Tatake, P.M. Kanthale, A.B. Pandit, AIChE 48 (7) (2002) 1542–1560.